

RESEARCH ARTICLE

Open Access

Ultrasound imaging in an experimental model of fatty liver disease and cirrhosis in rats

Andréia S Lessa¹, Bruno D Paredes², Juliana V Dias¹, Adriana B Carvalho², Luiz Fernando Quintanilha³, Christina M Takiya⁴, Bernardo R Tura⁵, Guilherme FM Rezende¹, Antonio C Campos de Carvalho^{2,5}, Célia MC Resende³, Regina CS Goldenberg^{2*}

Abstract

Background: Domestic dogs and cats are very well known to develop chronic hepatic diseases, including hepatic lipidosis and cirrhosis. Ultrasonographic examination is extensively used to detect them. However, there are still few reports on the use of the ultrasound B-mode scan in correlation with histological findings to evaluate diffuse hepatic changes in rodents, which represent the most important animal group used in experimental models of liver diseases. The purpose of this study was to determine the reliability of ultrasound findings in the assessment of fatty liver disease and cirrhosis when compared to histological results in Wistar rats by following up a murine model of chronic hepatic disease.

Results: Forty Wistar rats (30 treated, 10 controls) were included. Liver injury was induced by dual exposure to CCl₄ and ethanol for 4, 8 and 15 weeks. Liver echogenicity, its correlation to the right renal cortex echogenicity, measurement of portal vein diameter (PVD) and the presence of ascites were evaluated and compared to histological findings of hepatic steatosis and cirrhosis. Liver echogenicity correlated to hepatic steatosis when it was greater or equal to the right renal cortex echogenicity, with a sensitivity of 90%, specificity of 100%, positive and negative predictive values of 100% and 76.9% respectively, and accuracy of 92.5%. Findings of heterogeneous liver echogenicity and irregular surface correlated to liver cirrhosis with a sensitivity of 70.6%, specificity of 100%, positive and negative predictive values of 100% and 82.1% respectively, and accuracy of 87.5%. PVD was significantly increased in both steatotic and cirrhotic rats; however, the later had greater diameters. PVD cut-off point separating steatosis from cirrhosis was 2.1 mm (sensitivity of 100% and specificity of 90.5%). One third of cirrhotic rats presented with ascites.

Conclusion: The use of ultrasound imaging in the follow-up of murine diffuse liver disease models is feasible and efficient, especially when the studied parameters are used in combination. The potential implication of this study is to provide a non-invasive method that allows follow-up studies of fatty liver disease and cirrhosis of individual rats for pre-clinical drug or cell based therapies.

Background

Domestic dogs and cats are very well known to develop chronic hepatic diseases. Hepatic lipidosis (HL) or fatty liver is an important liver disease in cats. It is characterized by excess fat accumulation in the liver and seems to have no age, breed, or gender predilection [1,2]. HL is more common in obese or previously obese cats which have undergone brief periods

of anorexia or food deprivation [3]. Obesity in cats has been described as the most prevalent nutritional disease of the domestic cat in the United States of America [4]. Cornelius and DeNovo [5] reported HL as the underlying disease process in 12.5% of 80 cats with icterus.

Chronic hepatitis is a well-recognized problem in canine practice and affects dogs of many breeds [6]. However, knowledge of its etiology in dogs remains limited [7]. If chronic hepatitis is not treated, it can lead to the development of liver cirrhosis, which is characterized by architectural distortion of lobules,

* Correspondence: rcoeli@biof.ufrj.br

²Carlos Chagas Filho Biophysics Institute, Federal University of Rio de Janeiro, Av. Carlos Chagas Filho, 373, Bloco G, Sala G2-053, Rio de Janeiro, RJ, 21941-902, Brasil

bile duct hyperplasia, nodular regeneration and fibrosis [7].

Murine models of diffuse liver disease can be used as a base for pre-clinical studies [8]. Radiological methods such as ultrasound (US) brightness-mode (B-mode) imaging [1,2,9-11], duplex Doppler US [12], computed tomography perfusion [13] and magnetic resonance imaging (MRI) [14,15] have been used to detect and to follow-up experimental diffuse liver disease models. Additionally, Quintanilha *et al* [16] utilized US B-mode imaging in a longitudinal study to follow-up the effects of bone marrow stem cell therapy in rats submitted to liver injury, while Ju *et al* [17] prospectively tracked stem cells labeled with super paramagnetic particles transplanted intrasplenically in cirrhotic rats by MRI.

US examination has been extensively used to detect fatty liver disease and cirrhosis [18-20]. In cats and dogs, fatty liver disease can be diagnosed by the observation of an increased hepatic echogenicity, characterized by hyperechoic liver parenchymal texture compared to the renal cortex, and decreased visualization of deeper structures, such as the diaphragm and small peripheral vessels [21,22]. Cirrhosis, on the other hand, can be detected by a coarse and heterogeneous parenchymal echogenicity, irregular or nodular liver surface [21-23], focal regenerative nodules [21,24], decreased right lobe to caudate lobe ratio, indicating volume redistribution [25], and by indirect evidence of portal hypertension, such as increased portal vein diameter (PVD), presence of collateral vessels, splenomegaly and ascites [21,23,26].

Even though there are a number of studies that use US B-mode to evaluate liver diseases in rodents [9,27,28], few of these studies have statistically correlated US findings to the histological alterations present in liver parenchyma [29-31]. Lee *et al* [29] compared histopathological findings to the US B-mode quantitative parameter Mean Grey Level in CCl₄-induced liver cirrhosis, while Matsushashi *et al* [30] and Layer *et al* [31] correlated histology to Hepatic Ultrasound Speed and Texture Analysis respectively.

However, regardless of the fact that there is a correlation between quantitative B-mode methods and the histological features of cirrhosis, qualitative ultrasonography, which is the most common evaluation method of liver diseases in clinical practice both in animals and in humans, remains to be validated as a technique for the non-invasive diagnosis of such diseases in rodents. The purpose of our study was to determine the reliability of US qualitative findings in the assessment of fatty liver disease and cirrhosis in Wistar rats in comparison to histological results by following up a murine model of hepatic disease induced by dual exposure to CCl₄ and ethanol.

Methods

Animals

This investigation was performed in agreement with the Guide for Care and Use of Laboratory Animals [DHHS Publication No. (NIH) 85-23, revised 1996, Office of Science and Health Reports, Bethesda, MD 20892] and the authors have received approval from the Institutional Animal Care and Use Committee (protocol #021).

Female Wistar rats with 6 - 12 months of age, weighing between 160 - 180 g were housed at controlled temperature (23°C) with daily exposure to a 12:12 light-dark cycle.

Model of Experimental Cirrhosis

Animals (n = 40) were randomly divided into two groups: the Control group (n = 10) was fed with standard rat chow and water, and the Experimental group (n = 30) had chronic liver damage induced according to the protocol previously described by Dias *et al* [10], Quintanilha *et al* [16] and Carvalho *et al* [32]. Briefly, liver damage was induced with injections of a 20% solution of carbon tetrachloride (CCl₄) (1:5 in olive oil, dose of 0.05 mL/kg) intraperitoneally three times a week on alternate days combined with an alcoholic liquid diet in accordance with the AIN-93 guidelines [33] over 15 weeks.

Ultrasound Analysis

The Control and the Experimental groups were examined at the beginning of the experiment and after 4, 8 and 15 weeks of liver injury induction. Animals were anesthetized using ketamine (0.5 mL/kg) and xilazin (1 mL/kg) and had the abdomen shaved to reduce imaging artifacts in the ultrasonographic examination. A sound-conducting gel (Carbogel®, Brazil) was applied and an US examination was performed by two blinded expertise authors by consensus (reader 1, A.S.L., with 7 years experience, reader 10, C.M.C.R., with 26 years experience) by using a multifrequency linear transducer (7.5 to 10 MHz) and a Caris Plus® ultrasound equipment (Esaote, Italy). All imaging was performed in fundamental brightness mode (B-mode). Two-dimensional B-mode image plans were acquired with optimization of the gain and the time gain compensation settings, which were kept constant throughout the experiment. The acoustic focus was placed in the center of the target organ (liver) and in the largest transverse cross section of the spleen. The animals were examined in supine position to assess the liver and the portal vein, and in the right posterior oblique position to assess the spleen. These organs were evaluated by multiple transversal and longitudinal scans.

Ultrasonographic findings were analyzed based on our previous observations and on criteria for US diagnosis in humans according to the following classification:

A. Changes in the liver echogenicity, classified into four patterns: (1) homogeneous liver parenchyma with medium level echogenicity and a regular hepatic surface; (2) diffusely increased parenchymal echogenicity, reduced visualization of the diaphragm and small peripheral vessels in the liver with no change on liver surface; (3) discrete coarse and heterogeneous parenchymal echogenicity, dotted or slightly irregular liver surface; (4) extensive coarse and heterogeneous parenchymal echogenicity, irregular or nodular hepatic surface reflecting the presence of underlying regenerative nodules;

B. Inversion of the echographic relationship between the liver and the renal cortex. This finding was considered to be positive if the echogenicity of the liver parenchyma was greater or equal to that of the right renal cortex;

C. Increased PVD. It was measured in the mid-point of the main portal vein by using calipers of the scanner. PVD was considered to be abnormal if equal or greater than 2.1 mm;

D. Presence of ascites;

E. Spleen area. It was directly calculated by the US software after organ surface was delineated by the examiner.

Histological analysis

Rats from the Experimental and Control Groups were sacrificed on the 4th (n = 6), 8th (n = 7) and 15th (n = 17) week of the cirrhosis induction protocol. The liver was removed from the abdominal cavity for macroscopic post mortem analysis. For microscopic examination, liver tissue was fixed for 5 h in Gendre's solution followed by overnight incubation in 10% buffered formalin solution (pH 7.2) and embedded in paraffin. Liver samples were sectioned (5 μ m) and stained with hematoxylin and eosin (H&E) [34] or Sirius Red [35] according to standard protocols.

The histological diagnosis of fatty liver disease and cirrhosis was defined by a single blinded experienced pathologist based on the hepatic steatosis grading established by Ishak *et al* [36] and on the scoring system for hepatic fibrosis described by Plummer *et al* [37], respectively. Histology was used as the gold standard for both the diagnosis of fatty liver disease and cirrhosis and for the comparison with US results.

Statistical Analysis

The sensitivity, specificity, positive predictive value, negative predictive value and accuracy of the US findings for the detection of fatty liver disease and cirrhosis were calculated in comparison to the histological diagnosis [38]. PVD values were analyzed using analysis of variance (ANOVA) with Tukey's post-test for multiple comparisons. The value of $p < 0.01$ was considered statistically significant. Data are presented as mean \pm SD.

We also performed a Receiver Operating Characteristic (ROC) analysis of these data.

Results

Ultrasound Imaging

All animals were examined by US imaging in the beginning of experiment and after 4, 8 and 15 weeks of liver injury induction and the alterations found in the Experimental group were homogeneous in each examination time point. These alterations were represented by changes in liver echogenicity, in the relationship between liver parenchyma and renal cortex echogenicity, increased values of PVD and higher incidence of ascites when compared to the Control group (Table 1). A subset of animals in the Experimental group was sacrificed after 4 (n = 6) and 8 (n = 7) weeks of liver injury induction for histological studies, while the remaining animals (n = 17) were sacrificed after 15 weeks.

Histological Analysis

Control group showed a normal architecture with hepatocytes radially arranged in plates aligned to sinusoids converging to centrilobular veins and without evidence of fibrosis (Figure 1a). On the other hand, the Experimental group showed liver parenchymal alterations that correlated to the time of injury induction. After 4 weeks (n = 6), half of the animals presented with mild steatosis without fibrous septa and the other half showed mild to moderate steatosis with minimal focal pericellular and perivenular fibrosis (Figure 1b). After 8 weeks (n = 7), all the animals showed moderate to marked steatosis with some fibrous septa linking centrilobular veins to portal tracts, although liver parenchymal architecture was preserved (Figure 1c). After 15 weeks of induction (n = 17), all rats had macronodular cirrhosis, characterized by global architectural distortion and formation of regenerative nodules surrounded by collagen septa and containing some inflammatory infiltrate (Figure 1d). Mild to moderate steatosis was also present.

The prevalence of fatty liver disease among the 30 rats in the Experimental group was 100%, while the prevalence of cirrhosis was 56.7% (17 out of 30) when considering all the time points examined together. The lower prevalence of cirrhosis is expected since animals take longer periods of time to fully develop the histological alterations found in this disease. Accordingly, if we consider only the subset of animals that were injured for 15 weeks, the prevalence of cirrhosis was also 100%. No animals in the Control group presented with fatty liver disease or cirrhosis.

Correlation between Ultrasound Findings and Histological Diagnosis

Ultrasound and histological findings among the experimental groups were compared in the different time

Table 1 Ultrasound findings over the time of experiment observed in Experimental group compared to Control group

US findings/Time of experiment	Control Group at any time (n = 10)	Experimental Group		
		4 weeks (n = 6)	8 weeks (n = 7)	15 weeks (n = 17)
Homogeneous liver parenchyma of medium level echogenicity (pattern 1)	10	3	0	0
Diffusely increased parenchymal echogenicity (pattern 2)	0	3	3	0
Discrete coarsened and heterogeneous parenchyma (pattern 3)	0	0	4	5
Extensive coarsened and heterogeneous parenchyma (pattern 4)	0	0	0	12
L-Echo<R-Echo	10	3	0	0
L-Echo=R-Echo	0	2	4	8
L-Echo>R-Echo	0	1	3	9
Liver isoechoic nodule	0	0	0	2
Liver hypoechoic nodule	0	0	0	1
PVD< 2.1 mm	10	6	6	0
PVD ≥ 2.1 mm	0	0	1	17
Mild or transient ascites	0	0	0	2
Moderate or marked ascites	0	0	0	3

PVD: Portal Vein Diameter; L-Echo: Liver echogenicity; R-Echo: Renal cortex echogenicity.

points (Table 2, Figure 2). Samples of acquired US data used to perform correlation analysis can be seen in additional files (additional file 1, 2, 3, 4 and 5)

Liver echogenicity

The increase in liver echogenicity compared to right renal cortex echogenicity (L-Echo ≥ R-Echo) had a sensitivity of 90% (27 out of 30), specificity of 100% (10 out of 10), positive predictive value of 100% (27 out of 27), negative predictive value of 76.9% (10 out of 13) and accuracy of 92.5% (37 out of 40) for the detection of fatty liver disease and were well correlated with patterns

2 and 3 of liver echogenicity. The 3 rats which appeared to be normal in ultrasound imaging showed mild steatosis in microscopy. Control animals were all classified as pattern 1 and presented with normal liver parenchyma.

Moreover, pattern 4, characterized by extensive coarse and heterogeneous parenchymal echogenicity and irregular or nodular hepatic surface, was always associated with alteration of the echographic relationship between the liver and the right renal cortex. It had a sensitivity of 70.6% (12 out of 17), specificity of 100% (23 out of 23), positive predictive value of 100% (12 out of 12), negative

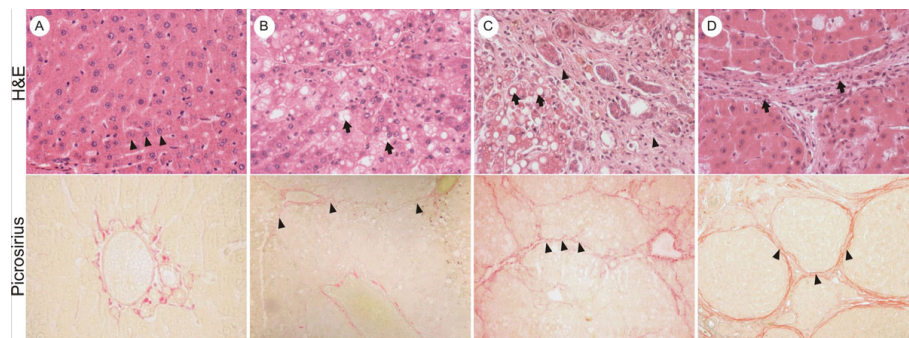


Figure 1 Histological findings observed over the experiment. (a) Microscopy of Control group (normal liver): Hematoxylin/Eosin (H&E) section (magnification 100x) shows hepatocytes radially arranged in plates aligned to sinusoids (arrowheads). Sirius red (magnification 100x) staining shows only vessels stained in red (portal triad - PT), which is a normal place of collagen deposit. (b) After 4 weeks of experiment: H&E section (magnification 100x) shows moderate steatosis (arrows). Sirius red (magnification 100x) staining shows focal perivenular and pericellular fibrosis (arrowheads) but preserved liver parenchymal architecture. Sirius red (magnification 100x) staining some fibrous septa linking centrolobular veins with portal tracts (arrowheads). (c) After 8 weeks of experiment H&E section (magnification 100x) shows moderate steatosis (arrows) with some fibrosis (arrowheads). Sirius red (magnification 100x) staining shows thick collagen septa (arrowheads) linking portal tracts, centrolobular veins, and portal tracts to centrolobular veins, forming regenerative nodules (RN). (d) After 15 weeks of protocol: H&E section (magnification 100x) shows macronodular cirrhosis, characterized by thick collagen septa, forming regenerative nodules, global architectural distortion, some inflammatory infiltrate (arrow) and steatosis. Sirius red (magnification 100x) staining shows thick collagen septa (arrowheads) linking portal tracts, centrolobular veins, and portal tracts to centrolobular veins, forming regenerative nodules (RN).

Table 2 Ultrasound findings compared to histological diagnosis

US findings	Histologic Diagnosis			
	Normal (n = 10)	Mild steatosis without fibrous septa (n = 3)	Mild to marked hepatic steatosis with various degrees of fibrosis but intact liver parenchymal architecture (n = 10)	Macronodular cirrhosis with hepatic steatosis (n = 17)
Pattern 1 L-Echo L-Echo < R-Echo	10	3	0	0
Pattern 1 L-Echo L-Echo ≥ R-Echo	0	0	0	0
Pattern 2, 3 or 4 L-Echo L-Echo < R-Echo	0	0	0	0
Pattern 2 L-Echo L-Echo ≥ R-Echo	0	0	6	0
Pattern 3 L-Echo L-Echo ≥ R-Echo	0	0	4	5
Pattern 4 L-Echo L-Echo ≥ R-Echo	0	0	0	12
Liver nodules	0	0	0	3 (regenerative nodules)
PVD < 2.1 mm	10	3	9	0
PVD ≥ 2.1 mm	0	0	1	17
Presence of ascites	0	0	0	5

L-Echo: Liver echogenicity; Pattern 1: normal echogenicity, pattern 2: diffusely increased echogenicity, pattern 3: slightly coarse echogenicity, and pattern 4: coarse and heterogeneous echogenicity; R-Echo: Renal cortex echogenicity; PVD: Portal Vein Diameter.

predictive value of 82.1% (23 out of 28) and accuracy of 87.5% (35 out of 40) for the detection of liver cirrhosis.

Portal Vein Diameter (PVD)

In the Experimental group, portal vein became wider and tortuous during hepatic disease development when compared to Control group (Figure 3). We analyzed PVD values among rats with cirrhosis, rats with steatosis and fibrosis and rats from the Control group. The results found were 2.2 ± 0.2 mm, 1.8 ± 0.2 mm and 1.5 ± 0.2 mm, respectively. PVD was significantly higher in cirrhotic rats and in rats with steatosis and fibrosis in comparison to the Control group (Figure 4), suggesting the presence of portal hypertension.

After Receiver Operating Characteristic (ROC) analysis of these data (Figure 5), we found that PVD values equal or greater than 2.1 mm had sensitivity of 100%, specificity of 90.5%, positive predictive value of 89.5% and negative predictive value of 100% for the detection of cirrhosis. Thus, this value can be considered a cut-off point for the diagnosis of cirrhosis in rats.

Presence of ascites and spleen measurements

Furthermore, the occurrence of ascites could be easily identified, even when small quantities of fluid were present in the abdominal cavity. This alteration was observed in 5 out of 17 cirrhotic rats (34%).

We also compared the spleen area among rats with cirrhosis, rats with steatosis and fibrosis and rats from the Control group. The results found were 1.19 ± 0.16

cm^2 , $1.16 \pm 0.14 \text{ cm}^2$ and $1.18 \pm 0.16 \text{ cm}^2$, respectively. There were no statistical differences among the three groups analyzed, indicating that splenomegaly was not a prominent feature in cirrhotic rats.

Discussion

In this work we demonstrated that qualitative ultrasound analysis is sensitive and specific enough to diagnose fatty liver disease and cirrhosis in rats and, therefore, can reliably substitute histological diagnosis in experimental liver disease models. Ultrasound imaging has many advantages, namely its low cost, extensive availability and the fact that it can be easily done in murine models. Only slight sedation and abdominal shaving are required, not demanding total immobility or apnea while obtaining the images [39], therefore, consisting in a low risk procedure. Moreover, it is an accurate, innocuous and non-invasive technique and it is the most commonly used method for the investigation of liver diseases in humans and small animals [1,18-21,40,41].

Although ultrasound is an essentially subjective diagnostic method, its validity as an imaging technique for liver evaluation has been extensively described in the literature for humans [40,42], dogs [21-23] and cats [1,21]. In our study, we focused our attention in a rodent model of liver disease, since these are the most commonly used models in pre-clinical studies [37,43-46]. The rat model was chosen because they are larger than mice, facilitating US imaging procedure.

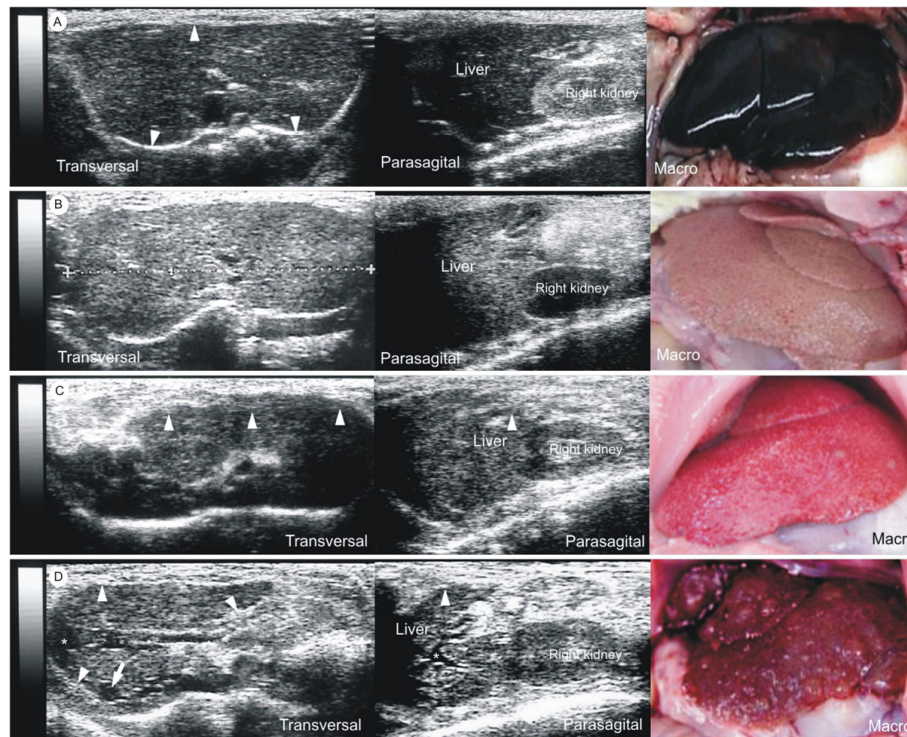


Figure 2 Correlation between ultrasound and histological findings. (a) Sonograms and macroscopy of Control group (normal liver): Transversal sonogram demonstrates homogeneous liver parenchyma, with medium level echogenicity and a regular hepatic surface (arrowheads). Parasagittal sonogram presents right renal cortex more echogenic than liver. Macroscopy shows smooth surface, brownish-red color and friable consistency. (b) Sonograms and macroscopy of fatty liver: Transversal sonogram presents diffusely increased parenchymal echogenicity. Parasagittal sonogram demonstrates hepatic echogenicity greater than that of right renal cortex. Macroscopy exhibits wrinkled surface, yellowish color and friable consistency. (c) Sonograms and macroscopy of liver carrying steatosis and fibrosis: Transversal sonogram shows discrete coarse and heterogeneous parenchymal echogenicity and the liver surface as a dotted or slightly irregular line (arrowheads). Parasagittal sonogram presents hepatic echogenicity equal to the right renal cortex echogenicity and a slightly irregular liver surface (arrowhead). Macroscopy shows a slightly irregular surface, pale red color and more rigid consistency. (d) Sonograms and macroscopy of cirrhotic liver: Transversal sonogram presents extensive coarse and heterogeneous parenchymal echogenicity, extremely irregular hepatic surface (arrowheads), a hypoechoic regenerative nodule (arrow) and mild ascites (*). Parasagittal sonogram shows hepatic echogenicity slightly greater than that of the right renal cortex, extremely irregular liver surface (arrowhead) and mild ascites (*). Macroscopy reveals extremely irregular surface, reflecting the presence of underlying regenerative nodules, reddish color and rigid consistency.

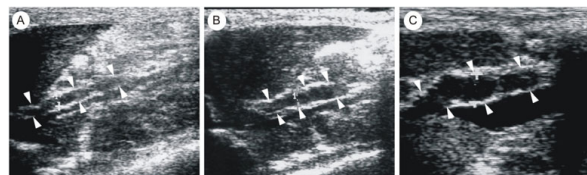
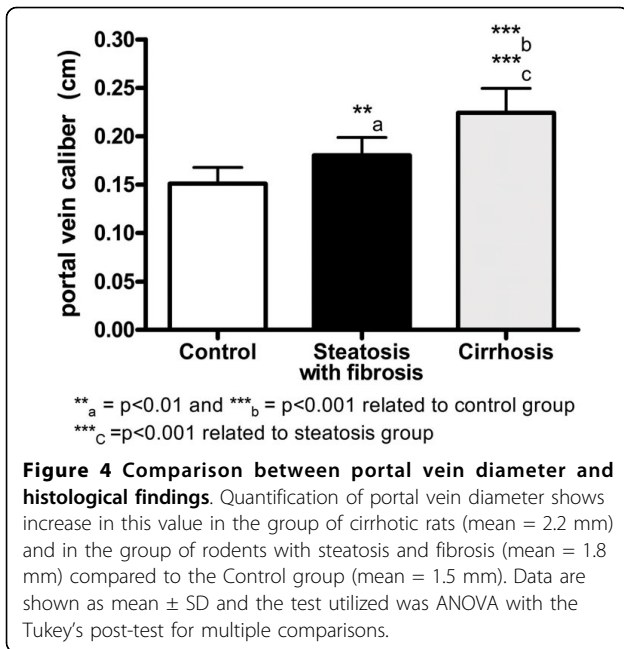


Figure 3 Portal vein widening over the experiment. (a) Parasagittal sonogram shows a straight and thin portal vein (diameter = 1.5 mm) in a Control group rat (arrowheads). (b) Parasagittal sonogram demonstrates a slightly tortuous and thin portal vein (diameter = 2.0 mm) in a rat with hepatic steatosis and fibrosis (arrowheads). (c) Parasagittal sonogram presents a tortuous and wide portal vein (diameter = 2.4 mm) in a cirrhotic rat (arrowheads).

Healthy rats showed homogeneous liver parenchyma, with medium level echogenicity and regular liver surface, as previously described in humans [47], dogs [21,23,48] and cats [2,21]. Liver echogenicity was lower in comparison to the right renal cortex, a finding that contrasts with humans [47], but is in accordance to what has been described in dogs [49]. In cats, renal cortical echogenicity varies in normal animals [50]. Fatty liver disease in rats was characterized by homogeneous and diffusely increased echogenicity ("bright liver"), equal or greater to the right renal cortex, reduced visualization of the diaphragm and of small peripheral vessels, and by no changes in liver surface, as described in humans [51], dogs [21,23], and cats [1,21].

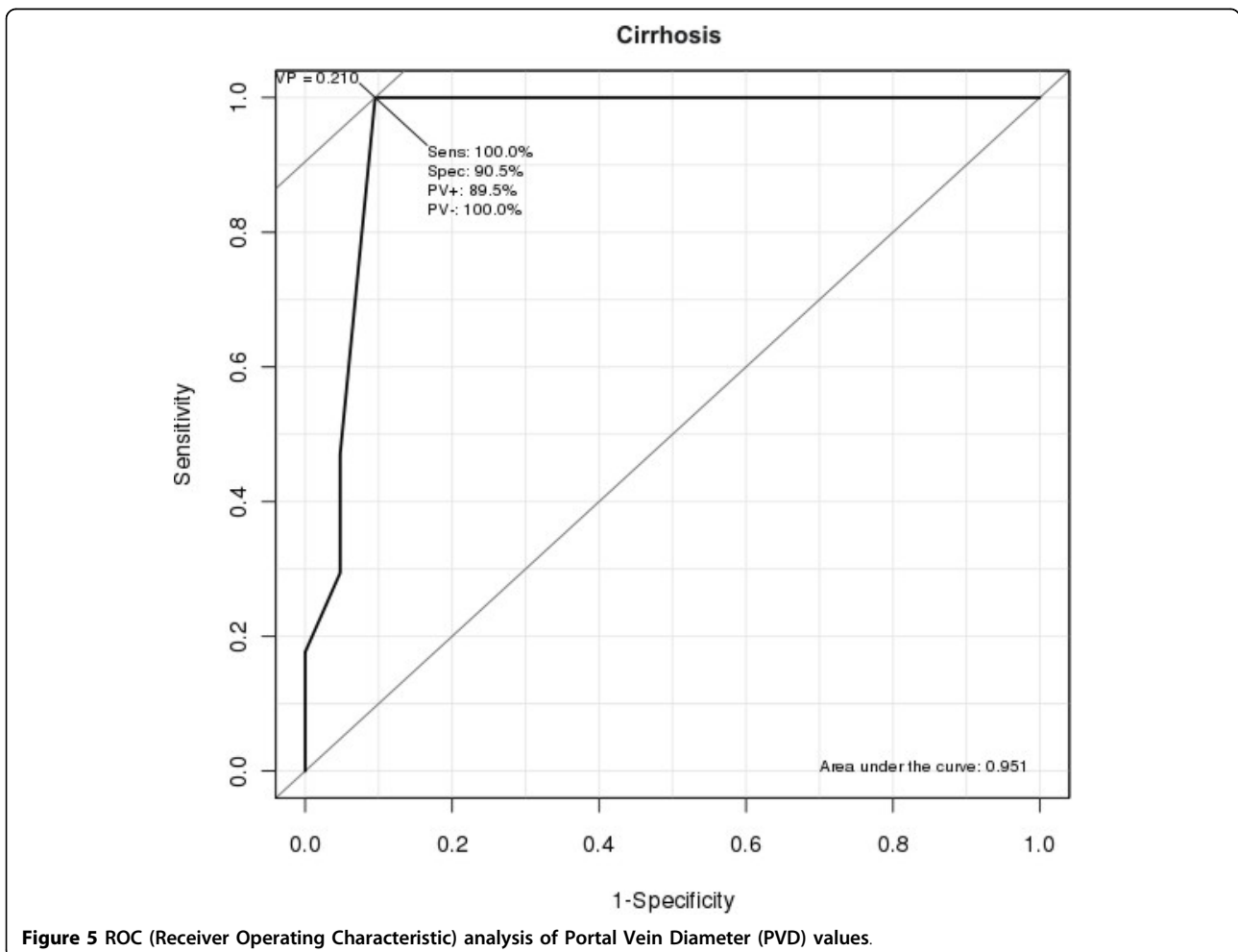
Liver echogenicity increases due to the presence of fatty infiltration and/or fibrosis [21,23], changing the



relation between liver and right renal cortex echogenicity [21,22]. This finding had high sensitivity (90%), specificity (100%), positive and negative predictive values (100% and 76.9%), and accuracy (92.5%) for the detection of fatty liver disease, values that were compatible with the ones previously described in the literature. The increased liver echogenicity has been reported to have sensitivity of 60 to 82% [1,23,52], specificity of 97 to 100% [1,52] and positive predictive value of 96 to 100% [1,52] for detection of fatty liver disease. However, it is important to exclude kidney diseases when utilizing this approach [23].

Three rats with mild hepatic steatosis appeared to be normal in US examination, which is also comparable to previous reports in the literature [23,52]. US has been reported to have sensitivity of 90 - 91% for the detection of moderate to marked steatosis, but its sensitivity decreases to 30 - 64% when steatosis is mild [23,52].

The finding of an extensive coarse and heterogeneous parenchyma associated to irregular or nodular hepatic surface proved to be relevant in the detection of



cirrhosis with sensitivity of 70.6%, specificity of 100%, positive predictive value of 100%, negative predictive value of 82.1% and accuracy of 87.5%, as seen in humans [40,53] and in dogs [23]. Its presence implied a definitive diagnosis of cirrhosis since there were no false negative results. Therefore, US imaging can consistently substitute histology to diagnose cirrhosis in rats, constituting a useful method to avoid unnecessary animal sacrifice or repeated liver biopsies when following long experimental protocols.

The evaluation of portal hypertension is also important to assess the severity of liver diseases [20,21,40] and one of its most important signs is the widening of the portal vein [20,21,47]. PVD was statistically different when comparing cirrhotic to non-cirrhotic rats ($p < 0.001$). An increase in its caliber when equal or superior to 2.1 mm can be considered a relevant ultrasound finding with sensitivity of 100%, specificity of 90.5%, positive predictive value of 89.5% and negative predictive value of 100% for the detection of cirrhosis. There was one false positive, a rat bearing liver steatosis with fibrosis. There were no false negatives since none of the rats with PVD lower than 2.1 mm were cirrhotic. Additionally, PVD measurements were unable to distinguish normal from steatotic livers because of the considerable overlap between PVD values encountered in normal rats compared to rats carrying steatosis and fibrosis. This fact is, nonetheless, expected since fatty liver disease does not lead to portal hypertension and, consequently, to the widening of the portal vein. Doppler evaluation of the portal vein was also tried, yet it was not possible due to technical difficulties. The caliper could not be stably positioned inside such a small vessel, we could not induce apnea and whirl flow was found even in normal rats, causing an oscillation between hepatopetal and hepatofugal flow.

The presence of ascites, which is also an important indicator of the severity of liver disease, could be detected even when the amount of fluid present in the peritoneal cavity was small, as previously reported by Vörös et al [54]. Among the imaging diagnostic methods, ultrasound is considered ideal for the study of ascites [6,21,23]. In our study, its presence invariably corresponded to cirrhosis in histology, although only 5 animals presented with ascites out of 17 cirrhotic rats. This was, however, expected since ascites is only observed when cirrhosis is decompensated. In addition, although splenomegaly should be expected in severe cirrhosis with portal hypertension, there were no statistical differences in splenic area among the three groups analyzed, indicating that splenomegaly was not a prominent feature in our study of cirrhotic rats.

Conclusion

The use of ultrasound imaging in the diagnosis of murine liver disease models is feasible and efficient, especially when different parameters (liver echogenicity and its correlation to that of the right renal cortex, PVD and the presence of ascites) are used in combination. The implication of this study is to certify that fatty liver disease and cirrhosis can be reliably diagnosed by a non-invasive method that allows adequate long-term follow-up, which is usually needed in pre-clinical drug or cell-based therapy studies.

Additional file 1: Ultrasound imaging of Control group (transversal and parasagittal views). The exam begins making transversal scanning, which shows homogeneous liver parenchyma, with medium level echogenicity and a regular hepatic surface. In the sequence, the parasagittal scanning shows right renal cortex more echogenic than liver. Author: Lessa AS. Length: 31 seconds. Size: 2.65 MB.
Click here for file
[<http://www.biomedcentral.com/content/supplementary/1746-6148-6-6-S1.MPG>]

Additional file 2: Ultrasound imaging of steatotic liver (transversal view). Transversal scanning shows diffusely increased parenchymal echogenicity. Author: Lessa AS. Length: 35 seconds. Size: 3.02 MB.
Click here for file
[<http://www.biomedcentral.com/content/supplementary/1746-6148-6-6-S2.MPG>]

Additional file 3: Ultrasound imaging of steatotic liver (parasagittal view). Parasagittal scanning shows hepatic echogenicity slightly greater than that of right renal cortex. Author: Lessa AS. Length: 10 seconds. Size: 0.39 MB.
Click here for file
[<http://www.biomedcentral.com/content/supplementary/1746-6148-6-6-S3.MPG>]

Additional file 4: Ultrasound imaging of cirrhotic liver (transversal view). Transversal scanning shows marked ascites, extensive coarse and heterogeneous parenchymal echogenicity and extremely irregular hepatic surface. Author: Resende CMC. Length: 35 seconds. Size: 3.06 MB.
Click here for file
[<http://www.biomedcentral.com/content/supplementary/1746-6148-6-6-S4.MPG>]

Additional file 5: Ultrasound imaging of cirrhotic liver (parasagittal view). Parasagittal scanning shows hepatic echogenicity equal to that of the right renal cortex, extremely irregular liver surface, tortuous and wide portal vein and marked ascites. Author: Resende CMC. Length: 70 seconds. Size: 6.06 MB.
Click here for file
[<http://www.biomedcentral.com/content/supplementary/1746-6148-6-6-S5.MPG>]

Acknowledgements

This study was supported in part by grants from the Council of Higher Education Improvement (Coordenação de Aperfeiçoamento de Pessoal de Nível Superior - CAPES-MEC), from the Brazilian Ministry of Science and Technology (Ministério de Ciência e Tecnologia - MCT-PRONEX), from the Foundation of Support for Research of the State of Rio de Janeiro (Fundação de Amparo à Pesquisa do Estado do Rio de Janeiro - FAPERJ), from the National Council of Scientific and Technological Development (Conselho Nacional de Desenvolvimento Científico e Tecnológico - CNPq), and from the Brazilian Ministry of Health (Ministério da Saúde - MS).

Author details

¹Department of Internal Medicine, School of Medicine, Federal University of Rio de Janeiro, Clementino Fraga Filho University Hospital, Rua Prof. Rodolpho Paulo Rocco, 255, Rio de Janeiro, 21941-913, Brasil. ²Carlos Chagas Filho Biophysics Institute, Federal University of Rio de Janeiro, Av. Carlos Chagas Filho, 373, Bloco G, Sala G2-053, Rio de Janeiro, RJ, 21941-902, Brasil. ³Department of Radiology, School of Medicine, Federal University of Rio de Janeiro, Clementino Fraga Filho University Hospital, Rua Professor Rodolpho Paulo Rocco, 255, Rio de Janeiro, 21941-913, Brasil. ⁴Department of Histology and Embryology, Institute of Biomedical Sciences, Federal University of Rio de Janeiro, Av. Carlos Chagas Filho, 373, Bloco F2-024, Rio de Janeiro, RJ, 21941-902, Brasil. ⁵National Institute of Cardiology, Rua das Laranjeiras, 374, 2º andar, Rio de Janeiro, RJ, 22240-006, Brasil.

Authors' contributions

BDP, LFQM, ABC, GFMR, ACCC and RCSG designed the study, performed the pilot studies and helped to draft the manuscript. ASL and CMCR carried out the ultrasonography and drafted the manuscript. BPD, JVD, CMT and BRT carried out analysis and interpretation of the data and helped to draft the manuscript. All authors revised and approved the final manuscript.

Competing interests

The authors declare that they have no competing interests.

Received: 7 August 2009

Accepted: 29 January 2010 Published: 29 January 2010

References

1. Yeager AE, Mohammed H: Accuracy of ultrasonography in the detection of severe hepatic lipidosis in cats. *Am J Vet Res* 1992, **53**:597-599.
2. Nicoll RG, O'Brien RT, Jackson MW: Qualitative ultrasonography of the liver in obese cats. *Vet Radiol Ultrasound* 1998, **39**:47-50.
3. Center AS, Crawford MA, Guida L, Erb HN, King J: A retrospective study of 77 cats with severe hepatic lipidosis: 1975-1990. *J Vet Intern Med* 1993, **7**:349-359.
4. Scarlett JM, Donoghue S, Saidla J, Wills J: Overweight cats: prevalence and risk factors. *Int J Obes Relat Metab Disord* 1994, **18**(Suppl 1):22-28.
5. Cornelius LM, DeNovo RC: Icterus in Cat. *Current veterinary therapy Philadelphia*: WB Saunders Co; 1983, 822-827.
6. Raffan E, McCallum A, Scase TJ, Watson PJ: Ascites is a negative prognostic indicator in chronic hepatitis in dogs. *J Vet Intern Med* 2009, **23**:63-66.
7. Sevelius E: Diagnosis and prognosis of chronic hepatitis and cirrhosis in dogs. *J Small Anim Pract* 1995, **36**:521-528.
8. Bujanda L, Hijona E, Larzabal M, Beraza M, Aldazabal P, Garcia-Urkieta N, Sarasqueta C, Cosme A, Irastorza B, Gonzalez A, Arenas JJ Jr: Resveratrol inhibits nonalcoholic fatty liver disease in rats. *BMC Gastroenterol* 2008, **8**:40.
9. de Lima VM, Oliveira CP, Alves VA, Chammas MC, Oliveira EP, Stefano JT, de Mello ES, Cerri GG, Carrilho FJ, Caldwell SH: A rodent model of NASH with cirrhosis, oval cell proliferation and hepatocellular carcinoma. *J Hepatol* 2008, **49**:1055-1061.
10. Dias JV, Paredes BD, Mesquita LF, Carvalho AB, Kozlowski EO, Lessa AS, Takiya CM, Resende CM, Coelho HS, Campos-de-Carvalho AC, Rezende GF, Goldenberg RC: An ultrasound and histomorphological analysis of experimental liver cirrhosis in rats. *Braz J Med Biol Res* 2008, **41**:992-999.
11. Feeney DA, Anderson KL, Ziegler LE, Jessen CR, Daubs BM, Hardy RM: Statistical relevance of ultrasonographic criteria in the assessment of diffuse liver disease in dogs and cats. *Am J Vet Res* 2008, **69**:212-221.
12. Nyland TG, Fisher PE: Evaluation of experimentally induced canine hepatic cirrhosis using duplex Doppler ultrasound. *Vet Radiol* 1990, **31**:189-194.
13. Guan S, Zhao WD, Zhou KR, Peng WJ, Mao J, Tang F: CT perfusion at early stage of hepatic diffuse disease. *World J Gastroenterol* 2005, **11**:3465-3467.
14. Kreft B, Dombrowski F, Block W, Bachmann R, Pfeifer U, Schild H: Evaluation of different models of experimentally induced liver cirrhosis for MRI research with correlation to histopathologic findings. *Invest Radiol* 1999, **34**:360-366.
15. Kim H, Booth CJ, Pinus AB, Chen P, Lee A, Qiu M, Whitlock M, Murphy PS, Constable RT: Induced hepatic fibrosis in rats: hepatic steatosis, macromolecule content, perfusion parameters, and their correlations—preliminary MR imaging in rats. *Radiology* 2008, **247**:696-705.
16. Quintanilha LF, Mannheimer EG, Carvalho AB, Paredes BD, Dias JV, Almeida AS, Gutfilen B, Barbosa da Fonseca LM, Resende CM, Rezende GF, Campos de Carvalho AC, Goldenberg RC: Bone marrow cell transplant does not prevent or reverse murine liver cirrhosis. *Cell Transplant* 2008, **17**:943-953.
17. Ju S, Teng GJ, Lu H, Zhang Y, Zhang A, Chen F, Ni Y: In vivo MR tracking of mesenchymal stem cells in rat liver after intrasplenic transplantation. *Radiology* 2007, **245**:206-215.
18. Bedogni G, Bellentani S, Miglioli L, Masutti F, Passalacqua M, Castiglione A, Tiribelli C: The Fatty Liver Index: a simple and accurate predictor of hepatic steatosis in the general population. *BMC Gastroenterol* 2006, **6**:33.
19. Hepburn MJ, Vos JA, Fillman EP, Lawitz EJ: The accuracy of the report of hepatic steatosis on ultrasonography in patients infected with hepatitis C in a clinical setting: a retrospective observational study. *BMC Gastroenterol* 2005, **5**:14.
20. Hong WD, Zhu QH, Huang ZM, Chen XR, Jiang ZC, Xu SH, Jin K: Predictors of esophageal varices in patients with HBV-related cirrhosis: a retrospective study. *BMC Gastroenterol* 2009, **9**:11.
21. Partington BP, Biller DS: Hepatic imaging with radiology and ultrasound. *Vet Clin North Am Small Anim Pract* 1995, **25**:305-335.
22. Mwanza T, Miyamoto T, Okumura M, Kadosawa T, Fujinaga T: Ultrasonography, biochemical and hematological profiles in liver disease caused by intravenous administration of dimethylnitrosamine in dogs. *Jpn J Vet Res* 1997, **45**:153-161.
23. Biller DS, Kantrowitz B, Miyabayashi T: Ultrasonography of diffuse liver disease. A review. *J Vet Intern Med* 1992, **6**:71-76.
24. Stowater CR, Lamb CH, Schelling SH: Ultrasonographic features of canine nodular hyperplasia. *Vet Radiol* 1990, **32**:268-271.
25. Giorgio A, Amoroso P, Lettieri G, Fico P, de Stefano G, Finelli L, Scala V, Tarantino L, Pierri P, Pesce G: Cirrhosis: value of caudate to right lobe ratio in diagnosis with US. *Radiology* 1986, **161**:443-445.
26. Lafortune M, Constantin A, Breton G, Legare AG, Lavoie P: The recanalized umbilical vein in portal hypertension: a myth. *AJR Am J Roentgenol* 1985, **144**:549-553.
27. Liao AH, Cheng YC, Weng CH, Tsai TF, Lin WH, Yeh SH, Yeh WC, Li PC: Characterization of malignant focal liver lesions with contrast-enhanced 40 MHz ultrasound imaging in hepatitis B virus X transgenic mice: a feasibility study. *Ultrasound Imaging* 2008, **30**:203-216.
28. Hanajiri K, Mitsui H, Maruyama T, Hashimoto N, Sata M, Omata M: Echographic detection of diethylnitrosamine-induced liver tumors in rats and the effect of the intratumoral injection of an inhibitor of c-Jun N-terminal kinase. *J Gastroenterol Hepatol* 2009, **24**:866-871.
29. Lee GP, Jeong WI, Jeong DH, Do SH, Kim TH, Jeong KS: Diagnostic evaluation of carbon tetrachloride-induced rat hepatic cirrhosis model. *Anticancer Res* 2005, **25**:1029-1038.
30. Matsuhashi T, Yamada N, Shinzawa H, Takahashi T: An evaluation of hepatic ultrasound speed in injury models in rats: correlation with tissue constituents. *J Ultrasound Med* 1996, **15**:563-570.
31. Layer G, Zuna I, Lorenz A, Zerban H, Haberkorn U, Bannasch P, Van Kaick G, R ath U: Computerized ultrasound B-scan texture analysis of experimental diffuse parenchymal liver disease: correlation with histopathology and tissue composition. *J Clin Ultrasound* 1991, **19**:193-201.
32. Carvalho AB, Quintanilha LF, Dias JV, Paredes BD, Mannheimer EG, Carvalho FG, Asensi KD, Gutfilen B, Fonseca LM, Resende CM, Rezende GF, Takiya CM, de Carvalho AC, Goldenberg RC: Bone marrow multipotent mesenchymal stromal cells do not reduce fibrosis or improve function in a rat model of severe chronic liver injury. *Stem Cells* 2008, **26**:1307-1314.
33. Reeves PG, Nielsen FH, Fahey GC Jr: AIN-93 purified diets for laboratory rodents: final report of the American Institute of Nutrition ad hoc writing committee on the reformulation of the AIN-76A rodent diet. *J Nutr* 1993, **123**:1939-1951.
34. Lacaz CS, Porto E, Martins JEC, Heins-Vaccari EM, Melo NT: *Tratado de Micologia* S o Paulo: Sarvier 1998.
35. Dolber PC, Spach MS: Conventional and confocal fluorescence microscopy of collagen fibers in the heart. *J Histochem Cytochem* 1993, **41**:465-469.
36. Ishak K, Baptista A, Bianchi L, Callea F, De Groote J, Gudat F, Denk H, Desmet V, Korb G, MacSween RN, Phillips MJ, Portmann BG, Poulsen H,

- Scheuer PJ, Schmid M, Thaler H: **Histological grading and staging of chronic hepatitis.** *J Hepatol* 1995, **22**:696-699.
37. Plummer JL, Hall PD, Ilsley AH, Cmielewski PL, Ahern MJ, Williams RA: **Dose-response relationships in hepatic injury produced by alcohol and carbon tetrachloride.** *Alcohol Clin Exp Res* 1994, **18**:1523-1526.
 38. Fletcher RH, Fletcher SW, Wagner EH: *Clinical Epidemiology: The Essentials* Philadelphia: Lippincott Williams & Wilkins 2005.
 39. Henson FM, Lamas L, Knezevic S, Jeffcott LB: **Ultrasonographic evaluation of the supraspinous ligament in a series of ridden and unridden horses and horses with unrelated back pathology.** *BMC Vet Res* 2007, **3**:3.
 40. Tchelepi H, Ralls PW, Radin R, Grant E: **Sonography of diffuse liver disease.** *J Ultrasound Med* 2002, **21**:1023-1032.
 41. Lamb CR: **Abdominal ultrasonography in small animals: examination of the liver, spleen and pancreas.** *J Small Anim Pract* 1990, **31**:5-8.
 42. Schalm SW: **The diagnosis of cirrhosis: clinical relevance and methodology.** *J Hepatol* 1997, **27**:1118-1119.
 43. Hall PD, Plummer JL, Ilsley AH, Cousins MJ: **Hepatic fibrosis and cirrhosis after chronic administration of alcohol and "low-dose" carbon tetrachloride vapor in the rat.** *Hepatology* 1991, **13**:815-819.
 44. Plummer JL, Hall PD, Cmielewski PL, Ilsley AH, Ahern MJ: **Alcohol/"Low-dose" carbon tetrachloride-induced cirrhosis in rats using different methods of alcohol feeding.** *Alcohol Clin Exp Res* 1994, **18**:1502-1505.
 45. Siegers CP, Völpel M, Scheel G, Younes M: **Effects of dithiocarb and (+)-catechin against carbon tetrachloride-alcohol-induced liver fibrosis.** *Agents Actions* 1982, **12**:743-748.
 46. Muñoz Torres E, Paz Bouza JL, Abad Hernandez MM, Alonso Martin MJ, Lopez Bravo A: **Experimental carbon tetrachloride-induced cirrhosis of the liver.** *Int J Tissue React* 1988, **10**:245-251.
 47. Dick R: **The liver and spleen.** *Textbook of radiology imaging* China: Churchill LivingstoneSutton D , 6 1998, 981-1028.
 48. England GCW: **Renal and hepatic ultrasonography in the neonatal dog.** *Vet Radiol Ultrasound* 1996, **37**:374-382.
 49. Ivancic M, Mai W: **Qualitative and quantitative comparison of renal vs. hepatic ultrasonographic intensity in healthy dogs.** *Vet Radiol Ultrasound* 2008, **49**:368-373.
 50. Drost WT, Henry GA, Meinkoth JH, Woods JP, Lehenbauer TW: **Quantification of hepatic and renal cortical echogenicity in clinically normal cats.** *Am J Vet Res* 2000, **61**:1016-1020.
 51. Mathiesen UL, Franzen LE, Aselius H, Resjo M, Jacobsson L, Foberg U, Fryden A, Bodemar G: **Increased liver echogenicity at ultrasound examination reflects degree of steatosis but not of fibrosis in asymptomatic patients with mild/moderate abnormalities of liver transaminases.** *Dig Liver Dis* 2002, **34**:516-522.
 52. Palmentieri B, de Sio I, La Mura V, Masarone M, Vecchione R, Bruno S, Torella R, Persico M: **The role of bright liver echo pattern on ultrasound B-mode examination in the diagnosis of liver steatosis.** *Dig Liver Dis* 2006, **38**:485-489.
 53. Colli A, Fraquelli M, Andreoletti M, Marino B, Zuccoli E, Conte D: **Severe liver fibrosis or cirrhosis: accuracy of US for detection-analysis of 300 cases.** *Radiology* 2003, **227**:89-94.
 54. Voros K, Albert M, Vetesi F, Harmat G, Binder K, Szaniszló F: **Hepatic ultrasonographic findings in experimental carbon tetrachloride intoxication of the dog.** *Acta Vet Hung* 1997, **45**:137-150.

doi:10.1186/1746-6148-6-6

Cite this article as: Lessa et al.: Ultrasound imaging in an experimental model of fatty liver disease and cirrhosis in rats. *BMC Veterinary Research* 2010 **6**:6.

**Submit your next manuscript to BioMed Central
and take full advantage of:**

- Convenient online submission
- Thorough peer review
- No space constraints or color figure charges
- Immediate publication on acceptance
- Inclusion in PubMed, CAS, Scopus and Google Scholar
- Research which is freely available for redistribution

Submit your manuscript at
www.biomedcentral.com/submit

